

# Divergent four-point dynamic density correlation function of a glassy colloidal suspension: a diagrammatic approach

Grzegorz Szamel

*Department of Chemistry, Colorado State University, Fort Collins, CO 80523*

(Dated: June 18, 2018)

We use a recently derived diagrammatic formulation of the dynamics of interacting Brownian particles [G. Szamel, *J. Chem. Phys.* **127**, 084515 (2007)] to study a four-point dynamic density correlation function. We re-sum a class of diagrams which separate into two disconnected components upon cutting a single propagator. The resulting formula for the four-point correlation function can be expressed in terms of three-point functions closely related to the three-point susceptibility introduced by Biroli *et al.* [*Phys. Rev. Lett.* **97**, 195701 (2006)] and the standard two-point correlation function. The four-point function has a structure very similar to that proposed by Berthier and collaborators [*Science* **310**, 1797 (2005), *J. Chem. Phys.* **126**, 184503 (2007)]. It exhibits a small wave vector divergence at the mode-coupling transition.

PACS numbers: 64.70.pv, 05.70.Ln

*Introduction* — It has become clear over the past decade that upon approaching the glass transition, the liquid’s dynamics not only get slower but also become increasingly heterogeneous [1]. Naturally, one of the very first questions that arose after the discovery of dynamic heterogeneities was that of their spatial extent. Indeed, some of the very first simulational studies of dynamic heterogeneities tried to estimate their size and showed that it increases upon cooling [2]. The discovery of growing dynamic heterogeneities posed a challenging problem for the mode-coupling theory [3, 4] of the glass transition. First, according to the standard formulation of this theory [3], the glass transition is supposed to be a small spatial scale phenomenon arising from a self-consistent caging of individual particles in their first solvation shells. Second, the mode-coupling theory relies upon a factorization approximation for a four-point dynamic density correlation function. Thus, it cannot even be expected to describe highly non-trivial spatiotemporal dependence of various four-point correlation functions that were introduced to monitor dynamic heterogeneities.

The above described problem was first addressed by Biroli and Bouchaud (BB) [5]. Inspired by an earlier study [6] of the so-called schematic mode-coupling equations, BB argued, using a field theoretical formulation of many-particle dynamics, that the mode-coupling theory should be understood as a saddle point approximation derived from an action functional. Furthermore, they argued that a four-point dynamic density correlation function could be calculated by inverting a second functional derivative of the same functional and that this procedure corresponds to a re-summation of ladder diagrams. They analyzed the convergence of the diagrammatic series and showed that their four-point function diverges at the transition point of the mode-coupling theory. In a very interesting later contribution Biroli, Bouchaud, Miyazaki and Reichman (BBMR) [7] used a more traditional, projection operator based [3] version of the mode-

coupling theory and showed that the matrix which determines the convergence of BB’s four-point function is exactly the same as the matrix which describes long wavelength properties of a certain three-point dynamic susceptibility describing the response of the intermediate scattering function to an external potential. Finally, in a pair of recent papers [8, 9] Berthier *et al.* used a field theoretical approach to argue that the most divergent part of the four-point dynamic density correlation function is given by, roughly speaking, a product of two three-point dynamic susceptibilities. According to Ref. [8] these three-point susceptibilities can be expressed in terms of ladder diagrams (in qualitative agreement with BBMR) and thus the most divergent part of the four-point function is represented by, roughly speaking, the sum of “squared ladder” diagrams [10].

The goal of this Letter is to analyze a four-point dynamic density correlation function of a glassy colloidal suspension. The reason for considering a colloidal system is twofold. First, experiments provide a wealth of information about the motion of individual colloidal particles and thus enable detailed tests of various theoretical predictions. Second, the simplest model of a colloidal suspension, a system of interacting Brownian particles, is technically simpler to study than a simple fluid. To analyze the four-point function we will use a recently derived [11] diagrammatic formulation of the dynamics of interacting Brownian particles. This formulation can use the same tools, *e.g.* re-summations of classes of diagrams, as a field theory based approach. It is, however, closer to the standard, projection operator based derivation of the mode-coupling theory.

In contrast to BB, we focus on singly connected diagrams, *i.e.* diagrams which separate into two disconnected components upon cutting through a single propagator. We will show that a sum of such diagrams results in a contribution to the four-point correlation function that diverges at the transition point of the mode-coupling

theory. The structure of this contribution is very similar to the structure of the most divergent part of the four-point function obtained by Berthier *et al.* [8, 12].

Since the derivation of the main result is rather tedious, we will first define our four-point function and present the main result. We will outline the derivation of this result in the latter part of this Letter.

*Four-point correlation function* — A number of different functions have been introduced to monitor dynamic heterogeneities [13]. In particular, two recent studies [14, 15, 16] used  $N \langle e^{-i\mathbf{k}\cdot(\mathbf{r}_1(t)-\mathbf{r}_1)} e^{i\mathbf{k}\cdot(\mathbf{r}_2(t)-\mathbf{r}_2)} \delta(\mathbf{r}-\mathbf{r}_{12}) \rangle$ , where  $\mathbf{r}_i(t)$  denotes the position of particle  $i$  at time  $t$ ,  $\mathbf{r}_i(0) \equiv \mathbf{r}_i$ ,  $\mathbf{r}_{12} = \mathbf{r}_1 - \mathbf{r}_2$ , and  $N$  is the number of particles. This function quantifies correlations between evolutions of two particles that were initially separated by  $|\mathbf{r}|$ . Its Fourier transform with respect to  $\mathbf{r}$  can be written as  $N \langle e^{-i\mathbf{k}\cdot(\mathbf{r}_1(t)-\mathbf{r}_2(t))} e^{i(\mathbf{k}-\mathbf{q})\cdot\mathbf{r}_{12}} \rangle$ . In this work, we consider a collective version of the latter expression,

$$S_4(\mathbf{k}; \mathbf{q}; t) = \frac{1}{N} \langle n_2(\mathbf{k}, -\mathbf{k}; t) n_2^*(\mathbf{k} - \mathbf{q}, -\mathbf{k} + \mathbf{q}) \rangle, \quad (1)$$

where  $n_2(\mathbf{k}_1, \mathbf{k}_2; t)$  denotes a projected two-particle density [17],

$$n_2(\mathbf{k}_1, \mathbf{k}_2; t) = (1 - \mathcal{P}_0 - \mathcal{P}_1) \sum_{i,j} e^{-i\mathbf{k}_1 \cdot \mathbf{r}_i(t) - i\mathbf{k}_2 \cdot \mathbf{r}_j(t)}. \quad (2)$$

In Eq. (2),  $\mathcal{P}_0$  and  $\mathcal{P}_1$  are projection operators onto the zero-particle and one-particle density, respectively [11]. In the following, we will often use an abbreviated notation and, *e.g.*, write  $n_2(\mathbf{k}_1, \mathbf{k}_2; t)$  as  $n_2(1, 2; t)$  or as  $n_2(t)$ ; in addition,  $n_2(t=0) \equiv n_2$ .

The projection operators in Eq. (2) remove a non-zero average value and a non-vanishing projection onto the one-particle density. The terms projected out do not contribute to the divergent part of  $S_4$ . Moreover, consistent usage of projected many-particle densities analogous to  $n_2$  has important technical advantages [11, 18]. In particular, bare inter-particle interactions are automatically renormalized by equilibrium correlation functions.

*Contribution to  $S_4$  due to singly connected diagrams* — In this work we focus on the diagrams which separate into two disconnected components upon cutting a single bond, with each component containing at least a single line of bonds from the initial time 0 to the final time  $t$  (the precise correspondence between  $S_4$  and the diagrams will be detailed below). The simplest diagram of this type is shown on the left in Fig. 1. In this diagram, bond  $\leftarrow$  represents a bare propagator and vertices  $\blacktriangleleft$ , and  $\blacktriangleright$  represent the left and right vertices, respectively [11]. Upon a re-summation, the bare singly connected diagram on the left in Fig. 1 is replaced by the diagram on the right of this figure. The latter diagram involves two new functions, closely related to the three-point susceptibility of BBMR, which are represented by  $\blacktriangleright$  and  $\blacktriangleleft$ , and full propagator represented by  $\leftarrow$ .

FIG. 1: Upon re-summation the simplest bare singly connected diagram on the left is replaced by a renormalized diagram on the right.

The main result of this note is the following formula for the part of  $S_4$  which becomes divergent at the mode-coupling transition; this formula results from an approximate re-summation indicated in Fig. 1:

$$S_4(\mathbf{k}; \mathbf{q}; t) = \frac{2}{nS(q)} \int \frac{d\omega}{2\pi} \chi_{-\mathbf{q}}^2(-\mathbf{k}; t; -\omega) \times G(q; \omega) \chi_{-\mathbf{q}}^1(\mathbf{k}; t; \omega) \quad (3)$$

Here  $G(q; \omega)$  is a Fourier transform of the full propagator,  $G(q; \omega) = \int dt e^{i\omega t} G(q; t)$ , and  $G(k; t)$  is defined in terms of the intermediate scattering function  $F(k; t)$ ,  $G(k; t) = \theta(t)F(k; t)/S(k)$ . Furthermore, in Eq. (3)  $\chi_{\mathbf{q}}^1(\mathbf{k}; t; \omega)$  and  $\chi_{\mathbf{q}}^2(\mathbf{k}; t; \omega)$  are three-point functions. They are related by  $\chi_{\mathbf{q}}^2(\mathbf{k}; t; -\omega) = e^{-i\omega t} \chi_{\mathbf{q}}^1(\mathbf{k} - \mathbf{q}; t; \omega)$ . Function  $\chi_{\mathbf{q}}^1(\mathbf{k}; t; \omega)$  satisfies the following equation of motion:

$$\int_0^t dt' (\delta(t-t') + M^{\text{irr}}(k; t-t')) \frac{\partial \chi_{\mathbf{q}}^1(\mathbf{k}; t'; \omega)}{\partial t'} + \frac{D_0 k^2}{S(k)} \chi_{\mathbf{q}}^1(\mathbf{k}; t; \omega) + \int_0^t dt' \int \frac{d\mathbf{k}'}{(2\pi)^3} \frac{n D_0 k}{|\mathbf{k} + \mathbf{q}|} \times v_{\mathbf{k}}(\mathbf{k}', \mathbf{k} - \mathbf{k}') \chi_{\mathbf{q}}^1(\mathbf{k}'; t-t'; \omega) F(|\mathbf{k} - \mathbf{k}'|; t-t') v_{\mathbf{k}+\mathbf{q}}(\mathbf{k}' + \mathbf{q}, \mathbf{k} - \mathbf{k}') \frac{\partial F(|\mathbf{k} + \mathbf{q}|; t')}{\partial t'} = \mathcal{S}_{\mathbf{q}}(\mathbf{k}; t; \omega) \quad (4)$$

In Eq. (4),  $D_0$  is the diffusion coefficient of an isolated Brownian particle,  $S(k)$  denotes the structure factor,  $n$  is the density and  $M^{\text{irr}}(k; t)$  is the irreducible [19] memory function. Moreover,  $v_{\mathbf{k}}(\mathbf{k}_1, \mathbf{k}_2) = \hat{\mathbf{k}} \cdot (c(k_1)\mathbf{k}_1 + c(k_2)\mathbf{k}_2)$  where  $c(k)$  is the Fourier transform of the direct cor-

relation function. The source term at the right-hand-side of Eq. (4),  $\mathcal{S}_{\mathbf{q}}(\mathbf{k}; t; \omega)$ , can be expressed in terms of the intermediate scattering function and equilibrium correlation functions. This term is regular and finite in the  $\mathbf{q} \rightarrow 0$  and  $\omega \rightarrow 0$  limits,  $\lim_{\mathbf{q} \rightarrow 0; \omega \rightarrow 0} \mathcal{S}_{\mathbf{q}}(\mathbf{k}; t; \omega) =$

$$nD_0S(0)k^2c(k)F(k;t).$$

As explained below, the re-summation leading to Eqs. (3-4) involves an approximation which is similar to the approximation used in the diagrammatic derivation of the mode-coupling theory [11]. Thus, to be consistent we replace the full  $G$ ,  $F$  and  $M^{\text{irr}}$  in Eqs. (3-4) by their approximate forms calculated using the mode-coupling equations. Specifically, we assume the standard mode-coupling relation which expresses  $M^{\text{irr}}$  in terms of  $F$ 's,  $M^{\text{irr}}(k;t) = (nD_0/2) \int (d\mathbf{k}'/(2\pi)^3) v_{\mathbf{k}}^2(\mathbf{k}', \mathbf{k} - \mathbf{k}') F(k'; t) F(|\mathbf{k} - \mathbf{k}'|; t)$ .

At this point we note that evolution operator on the left-hand-side of Eq. (4) with the mode-coupling expression for  $M^{\text{irr}}$  is exactly the same as the overdamped version of the evolution operator derived by BBMR for their three-point susceptibility. Indeed, the only difference between Eq. (4) and the overdamped version of the equation of motion (2) of Ref. [7] is the source term. Moreover, BBMR emphasized that all of their qualitative conclusions are independent of the precise structure of the source term. Thus, we conjecture that our three-point functions  $\chi_{\mathbf{q}}^1(\mathbf{k}; t; \omega)$  and  $\chi_{\mathbf{q}}^2(\mathbf{k}; t; \omega)$  have the same scaling behavior as  $\chi_{\mathbf{q}}(\mathbf{k}; t)$  of Ref. [7]. In particular, these functions exhibit a small wave vector divergence upon approaching the mode-coupling transition.

Furthermore, we note that Eq. (3) has the same general structure as the formula derived by Berthier *et al.* (see Eq. (56) of Ref. [8]) [20]. Thus, we are lead to the same conclusion: the divergence of the four-point dynamic density correlation function is intimately connected to and in fact driven by the divergence of the three-point function.

*Derivation* — We consider the time-dependent correlation function of the projected two-particle density,  $\langle n_2(1, 2; t) n_2^*(3, 4) \rangle$ . For a specific set of wave vectors this function is proportional to  $S_4$ : in the thermodynamic limit we get  $\langle n_2(\mathbf{k}, -\mathbf{k}; t) n_2^*(\mathbf{k} - \mathbf{q}, \mathbf{k}') \rangle = n^2 S_4(\mathbf{k}; \mathbf{q}; t) (2\pi)^3 \delta(\mathbf{k} + \mathbf{q} - \mathbf{k}')$ .

Following Ref. [11], it is possible to derive a hierarchy of equations describing the time evolution of  $\langle n_2(t) n_2^* \rangle$ . This hierarchy can be rewritten as a hierarchy of integral equations which can be solved by iteration. The solution can be represented in terms of diagrams consisting of the bare propagator,  $G_0(k; t) = \theta(t) \exp(-D_0 k^2 t / S(k))$ , represented by  $\longleftarrow$ , and three vertices, the left vertex,  $\mathcal{V}_{12}$ , represented by  $\llcorner$ , the right vertex,  $\mathcal{V}_{21}$ , represented by  $\lrcorner$ , and the four-leg vertex,  $\mathcal{V}_{22}$ , represented by  $\times$ . The vertices represent renormalized inter-particle interactions; they involve the direct correlation function and the structure factor rather than a bare interaction potential (see Eqs. (55-57) of Ref. [11]).

The diagrams contributing to  $\langle n_2(t) n_2^* \rangle$  separate into two classes: disconnected and connected ones. For  $q \neq 0$  only the latter diagrams contribute to  $S_4(\mathbf{k}; \mathbf{q}; t)$ . Here, we only consider singly connected diagrams. A singly connected diagram is a connected diagram which sepa-

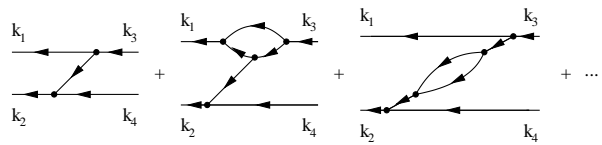


FIG. 2: The first few diagrams in the diagrammatic series for  $\langle n_2(\mathbf{k}_1, \mathbf{k}_2; t) n_2^*(\mathbf{k}_3, \mathbf{k}_4) \rangle^{\text{scn}}$ .

rates into two disconnected components upon cutting a single  $G_0$  bond, with each component containing at least a single line of bonds from the initial time 0 to the final time  $t$ . The first few such diagrams are shown in Fig. 2.

It is convenient to formulate the diagrammatic expansion for the singly connected part of  $\langle n_2(t) n_2^* \rangle$  divided by  $n^2 S(3) S(4)$ . For brevity, we will denote this function by  $\langle n_2(t) n_2^* \rangle^{\text{scn}}$ . In the diagrams contributing to it, we refer to the leftmost and the rightmost bare propagators as the left roots and the right roots, respectively, and to the other bare propagators as bonds. The roots are labeled by wave vectors and the bonds are unlabeled. It can be showed that  $\langle n_2(t) n_2^* \rangle^{\text{scn}}$  is the sum of all topologically different [11], singly connected diagrams with two left roots, two right roots,  $G_0$  bonds, and  $\mathcal{V}_{12}$ ,  $\mathcal{V}_{21}$ , and  $\mathcal{V}_{22}$  vertices. To evaluate a diagram one assigns wave vectors to bonds and integrates over these wave vectors (with a  $(2\pi)^{-3}$  factor for each integration), integrates over all intermediate times, and divides the result by a symmetry number [11] of the diagram; diagrams with odd and even numbers of  $\mathcal{V}_{22}$  vertices contribute with overall negative and positive signs, respectively.

To re-sum singly connected diagrams we first note that the sum of all the “connecting parts” in diagrams in Fig. 2 gives the full propagator  $G(q; t)$  [21]. The sums of the two remaining parts of singly connected diagrams are related to each other by a symmetry operation and thus we have to evaluate only one of them.

We define  $X_3^1(\mathbf{k}_1, \mathbf{q}; \mathbf{k}_3; t, t')$  as the sum of all connected, topologically different diagrams with one left root, one right root and one *left* side root (the left side root originates from a left “dangling” end of the right vertex,  $\mathcal{V}_{21}$ , or from a left “dangling” end of four-leg vertex,  $\mathcal{V}_{22}$ ). The first few diagrams contributing to  $X_3^1$  are shown in Fig. 3.

The last step in the re-summation is the derivation of a self-consistent equation for function  $X_3^1$  shown in Fig. 4. In this figure,  $\blacktriangleright$  represents function  $X_3^1$ , a thick bond  $\longleftarrow$  represents the full propagator  $G(k; t)$  and  $\circ$  represents the *reducible* memory matrix [11]. Here, we will only argue that equation in Fig. 4 is plausible [21]. Re-summation of diagrams similar to the first and second diagrams in Fig. 3 results in first diagram at the right-hand-side of diagrammatic equation in Fig. 4. Re-summation of diagrams similar to the third diagram in Fig. 3 results in the second diagram at the right-hand-side of Fig. 4. Re-summation of diagrams similar to the

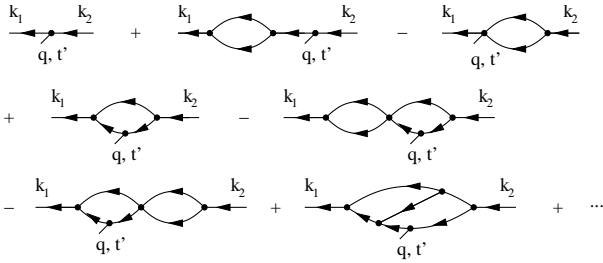


FIG. 3: The first few diagrams in the diagrammatic expansion for  $X_3^1(\mathbf{k}_1, \mathbf{q}; \mathbf{k}_2; t, t')$ . Note that the third, fifth and sixth diagrams, which contain a single  $\mathcal{V}_{22}$  vertex, contribute with a negative sign.

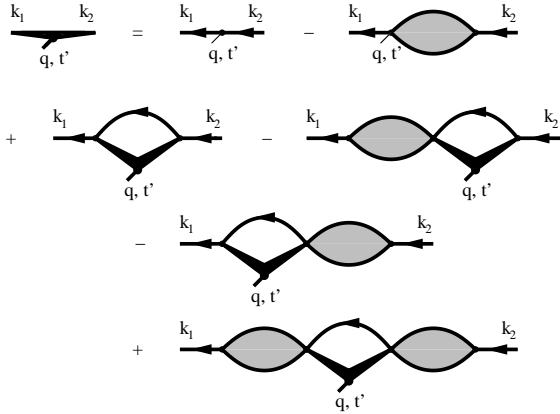


FIG. 4: Diagrammatic self-consistent equation for function  $X_3^1(\mathbf{k}_1, \mathbf{q}; \mathbf{k}_2; t, t')$ .

fourth diagram in Fig. 3 results in the third diagram at the right-hand-side of Fig. 4. Re-summations of diagrams similar to the fifth and sixth diagrams in Fig. 3 result in the fourth and fifth diagrams at the right-hand-side of Fig. 4, respectively. Diagrams similar to the seventh diagram in Fig. 3 are neglected. As mentioned above, diagrams neglected in our re-summation resemble diagrams which are neglected in the approximation leading to the mode-coupling expression for  $M^{\text{irr}}$  [11].

Parenthetically, diagrams resulting from the self-consistent equation showed in Fig. 4 could be written as ladder diagrams. However, these ladder diagrams would be quite unusual in that their beams would correspond to time running in opposite directions.

Next, we define three-point function  $\chi_{\mathbf{q}}^1(\mathbf{k}; t; t')$  in terms of  $X_3^1$ :  $X_3^1(\mathbf{k}, \mathbf{q}; \mathbf{k}'; t, t') = \chi_{\mathbf{q}}^1(\mathbf{k}; t; t')(2\pi)^3 \delta(\mathbf{k} + \mathbf{q} - \mathbf{k}')$ . We introduce its frequency dependent version  $\chi_{\mathbf{q}}^1(\mathbf{k}; t; \omega) = \int_0^t dt' e^{i\omega t'} \chi_{\mathbf{q}}^1(\mathbf{k}; t; t')$ . It can be showed that the self-consistent equation for  $X_3^1$  showed in Fig. 4 is equivalent to the equation of motion (4) for the frequency dependent function  $\chi_{\mathbf{q}}^1(\mathbf{k}; t; \omega)$ . A symmetry relation mentioned above results in the relation between  $\chi^1$  and  $\chi^2$  given below Eq. (3). Finally, we express the sum of singly connected diagrams in terms of  $G$ ,  $\chi^1$  and  $\chi^2$ , and we get expression (3) for the part of  $S_4$  which ex-

hibits small wave vector divergence at the mode-coupling transition.

*Conclusions* — We have showed that the contribution to the four-point dynamic density correlation function of a glassy colloidal suspension due to diagrams which separate into two disconnected components upon cutting a single propagator can be expressed in terms of three-point functions which diverge at small wave vectors. Thus, the four-point correlation function of a glassy colloidal suspension exhibits a small wave vector divergence. In addition, we have derived an explicit formula for the dominant part of the four-point function.

*Acknowledgments* — I gratefully acknowledge the support of NSF Grant No. CHE 0517709.

- [1] For reviews of experimental evidence of dynamic heterogeneities see, *e.g.* M. Ediger, *Annu. Rev. Phys. Chem.* **51**, 99 (2000) and R. Richert, *J. Phys. Cond. Matt.* **14** R703 (2002). For a recent review of simulational evidence see H.C. Andersen, *PNAS* **102**, 6686 (2005).
- [2] W. Kob *et al.*, *Phys. Rev. Lett.* **79**, 2827 (1997); C. Donati, S.C. Glotzer, and P.H. Poole, *Phys. Rev. Lett.* **82**, 5064 (1999).
- [3] W. Götze, in *Liquids, Freezing and Glass Transition*, J.P. Hansen, D. Levesque, and J. Zinn-Justin, eds. (North-Holland, Amsterdam, 1991).
- [4] S.P. Das, *Rev. Mod. Phys.* **76**, 785 (2004).
- [5] G. Biroli and J.-P. Bouchaud, *Europhys. Lett.* **67**, 21 (2004).
- [6] S. Franz and G. Parisi, *J. Phys. Cond. Matt.* **12**, 6335 (2000).
- [7] G. Biroli, J.-P. Bouchaud, K. Miyazaki, and D.R. Reichman, *Phys. Rev. Lett.* **97**, 195701 (2006).
- [8] L. Berthier *et al.*, *J. Chem. Phys.* **126**, 184503 (2007).
- [9] L. Berthier *et al.*, *J. Chem. Phys.* **126**, 184504 (2007).
- [10] The sum of BB's ladder diagrams enters as a subdominant contribution.
- [11] G. Szamel, *J. Chem. Phys.* **127**, 084515 (2007).
- [12] L. Berthier *et al.*, *Science* **310**, 1797 (2005).
- [13] See, *e.g.*, S.C. Glotzer, V.N. Novikov, T.B Schröder, *J. Chem. Phys.* **119**, 7372 (2003) and N. Lačević, and S.C. Glotzer, *J. Phys. Cond. Matt.* **15**, S2437 (2003).
- [14] E. Flenner and G. Szamel, *J. Phys. Cond. Matt.* **19**, 205125 (2007).
- [15] D. Chandler *et al.*, *Phys. Rev. E* **74**, 051501 (2006).
- [16] A related function was used by L. Berthier [*Phys. Rev. E* **69**, 020201(R) (2004)] and S. Whitelam, L. Berthier, and J.P. Garrahan [*Phys. Rev. Lett.* **92**, 187505 (2004)].
- [17] For brevity, we use the term density for the Fourier transform of the density.
- [18] H.C. Andersen, *J. Phys. Chem. B* **106**, 8326 (2002); *ibid.*, **107**, 10226 (2003); *ibid.*, **107**, 10234 (2003).
- [19] B. Cichocki and W. Hess, *Physica A* **141**, 475 (1987).
- [20] The detailed form of (3) cannot be compared with results of Refs. [8, 9, 12] since the latter works did not present an explicit formula for the four-point function at  $q \neq 0$ .
- [21] The details will be presented elsewhere.